

Spectral components and their contributions to the 1.5 μm emission bandwidth of erbium-doped oxide glass

Jiangting Sun, Jiahua Zhang, Yongshi Luo, Jiuling Lin, and Hongwei Song

Citation: *J. Appl. Phys.* **94**, 1325 (2003); doi: 10.1063/1.1586958

View online: <http://dx.doi.org/10.1063/1.1586958>

View Table of Contents: <http://jap.aip.org/resource/1/JAPIAU/v94/i3>

Published by the [American Institute of Physics](#).

Related Articles

Mechanism of the enhancement of mid-infrared emission from GeS₂-Ga₂S₃ chalcogenide glass-ceramics doped with Tm³⁺

Appl. Phys. Lett. **100**, 231910 (2012)

Phase evolution and room-temperature photoluminescence in amorphous SiC alloy

J. Appl. Phys. **111**, 103526 (2012)

Silicon nanocluster sensitization of erbium ions under low-energy optical excitation

J. Appl. Phys. **111**, 094314 (2012)

Energy transfer and energy level decay processes in Tm³⁺-doped tellurite glass

J. Appl. Phys. **111**, 063105 (2012)

Green and red emission for (K_{0.5}Na_{0.5})NbO₃:Pr ceramics

J. Appl. Phys. **111**, 046102 (2012)

Additional information on J. Appl. Phys.

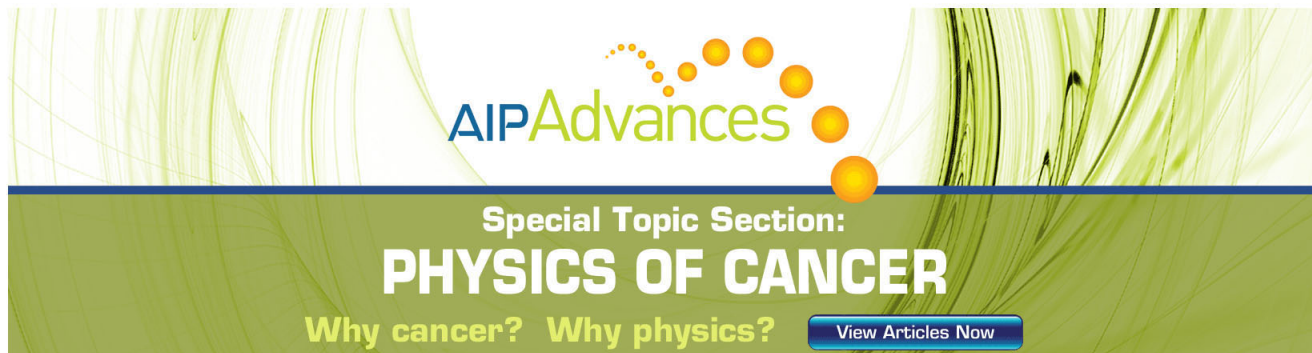
Journal Homepage: <http://jap.aip.org/>

Journal Information: http://jap.aip.org/about/about_the_journal

Top downloads: http://jap.aip.org/features/most_downloaded

Information for Authors: <http://jap.aip.org/authors>

ADVERTISEMENT



AIP Advances

Special Topic Section:
PHYSICS OF CANCER

Why cancer? Why physics? [View Articles Now](#)

Spectral components and their contributions to the 1.5 μm emission bandwidth of erbium-doped oxide glass

Jiangting Sun, Jiahua Zhang,^{a)} Yongshi Luo, Jiuling Lin, and Hongwei Song
*Key Laboratory of Excited State Processes, Changchun Institute of Optics, Fine Mechanics and Physics,
 Chinese Academy of Sciences, Changchun 130022, People's Republic of China*

(Received 2 January 2003; accepted 7 May 2003)

In this article, the 1.5 μm emission spectra corresponding to the ${}^4I_{13/2} \rightarrow {}^4I_{15/2}$ transition of Er^{3+} in oxide glass are studied within the temperature from 11 to 300 K. The spectral components emitting from the lowest and upper Stark levels of the ${}^4I_{13/2}$ state are analyzed and separated. The effect of the spectral components on the 1.5 μm emission bandwidth is investigated. The results indicate that to search a host with higher spontaneous emission probability of the upper Stark levels of the ${}^4I_{13/2}$ state for Er^{3+} ions is very important to broadening of the 1.5 μm emission band of Er^{3+} . An equivalent model of the four-level system is presented and applied to explain the spectral shape and temperature characteristics of the 1.5 μm emission band. According to the theory of McCumber, we transform the absorption spectrum into the emission spectrum, the shape of which fits well to that measured. © 2003 American Institute of Physics. [DOI: 10.1063/1.1586958]

I. INTRODUCTION

The erbium-doped fiber amplifier (EDFA), utilizing the emission transition ${}^4I_{13/2} \rightarrow {}^4I_{15/2}$ of Er^{3+} , is a key element of the 1.5 μm window telecommunication system. Due to the rapid increase of information capacity and the need for flexible networks, there is an urgent demand for optical amplifiers with a wide and flat gain spectrum in the telecommunication window, to be used in the wavelength-division-multiplexing (WDM) network system. The EDFA utilized at present is made of Er^{3+} -doped silica glass, which shows a narrow emission band at 1.55 μm resulting in narrow gain spectra with a bandwidth around 30 nm. The study on spectral broadening of 1.5 μm emission of Er^{3+} -doped various glasses, therefore, has been paid great attention.¹⁻⁹ The ${}^4I_{13/2} \rightarrow {}^4I_{15/2}$ emission spectrum is composed of spectral components originating from the transitions between the Stark splitting levels of ${}^4I_{13/2}$ and that of ${}^4I_{15/2}$ multiplets. The spectral intensities and positions of these components basically determine the 1.5 μm emission bandwidth. To identify these components and understand their contributions to spectral broadening is obviously helpful to designing materials with the 1.5 μm broad band. Jha and co-workers⁴ analyzed the spectral components of 1.5 μm emission in Er^{3+} -doped tellurite glasses by fitting the emission spectra with Voigtian shapes. The electronic transitions corresponding to the spectral components were discussed, but not determined precisely due to the lack of low temperature photoluminescence data.

In this article, we prepared an oxide glass based on B_2O_3 , Na_2O , Bi_2O_3 , and Y_2O_3 oxides as the host for Er^{3+} ions. The 1.5 μm emission spectra are studied within the temperature from 11 to 300 K. The spectral components of the transitions from the lowest and upper Stark levels of the

${}^4I_{13/2}$ state to the ground state are separated and identified, respectively. The contributions of the spectral components to broadening of the 1.5 μm emission band are discussed. An equivalent model of the four-level system is presented to describe the spectral shape of the ${}^4I_{13/2} \rightarrow {}^4I_{15/2}$ transition. According to the theory of McCumber, the absorption spectrum is transformed into the emission spectrum, the shape of which fits well to that experimentally measured.

II. EXPERIMENT

Glass in the composition of $60\text{B}_2\text{O}_3 - 30\text{Na}_2\text{O} - 5\text{Bi}_2\text{O}_3 - 5\text{Y}_2\text{O}_3 - 0.5\text{Er}_2\text{O}_3$ (in mol %) is prepared by melting well-mixed powders in a platinum crucible at 1350 °C for 1.5 h, then quenched into a preheated brass mold to form glass. The quenched sample is annealed around 500 °C for 24 h, then the obtained glass was cut and polished into $15 \times 15 \times 4.6 \text{ mm}^3$ size.

Emission spectra in the range of 1400–1700 nm are measured by using a Spex 1269 spectrometer with spectral resolution of 1 nm under the excitation of 980 nm light from a diode laser. Absorption spectra are measured by using a Perkin-Elmer Lambda 9 spectrometer. Different temperatures are obtained by using a helium gas cycling refrigerator.

III. RESULTS AND DISCUSSION

A. Analysis of emission spectra at different temperature

Figure 1 shows the emission spectra of the transition from the ${}^4I_{13/2}$ state to the ${}^4I_{15/2}$ state multiplets, where the area under the emission spectral profile is normalized. The emission spectra are composed of four spectral bands, labeled by a' , a , b' , and b , and the peaks of which are located at about 1500, 1529, 1555, and 1600 nm, respectively. At lower temperature of 11 K, there are only two bands, a and b , in the emission spectra. With increasing temperature, bands a and b decrease while bands a' and b' begin to appear and

^{a)} Author to whom correspondence should be addressed; electronic mail: zjiahua@public.cc.jl.cn

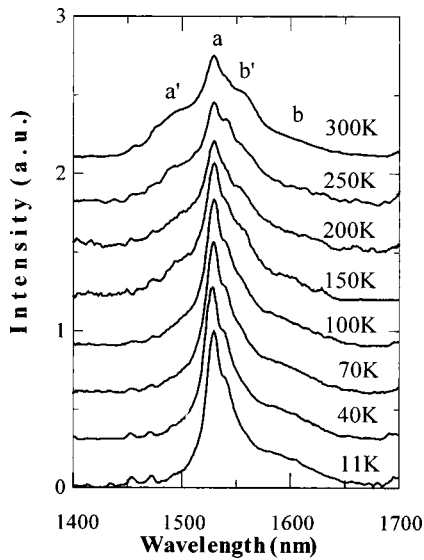


FIG. 1. Emission spectra of the ${}^4I_{13/2} \rightarrow {}^4I_{15/2}$ transition in the sample at temperatures from 11 to 300 K. The area under the spectra is normalized.

grow up. According to the temperature characteristics of these bands, we attribute bands *a* and *b* to the transition from the lowest Stark level of ${}^4I_{13/2}$ multiplets to the ${}^4I_{15/2}$ ground state, bands *a'* and *b'* to the transition from the upper Stark levels of ${}^4I_{13/2}$ state to the ground state. The bandwidth of the emission spectra is increased due to the growth of bands *a'* and *b'* with raising temperature. As illustrated in Fig. 1, with the increase of temperature from 11 to 300 K the emission spectral bandwidth, the full width at half maximum (FWHM), increases from 27 to 60 nm.

The emission spectra of the transition from the ${}^4I_{13/2}$ state to the ${}^4I_{15/2}$ state for Er^{3+} ions at temperature *T* can be expressed as

$$F(T, \lambda) = C \sum_{i=0}^m \gamma_i a_i f_i(\lambda), \quad (1)$$

where γ_i is the transition rate from the *i*th Stark level of the ${}^4I_{13/2}$ state to the ${}^4I_{15/2}$ state. a_i and $f_i(\lambda)$ are the population and the emission spectral distribution function of the *i*th Stark level, respectively, with $\int f_i(\lambda) d\lambda = 1$. *C* is a constant for normalization. According to Boltzman distribution, the population of the *i*th Stark level of the ${}^4I_{13/2}$ state is expressed as

$$a_i = \frac{g_i e^{-\Delta E_i/kT}}{\sum_{i=0}^m g_i e^{-\Delta E_i/kT}}, \quad (2)$$

where ΔE_i is the energy separation between the *i*th and the lowest Stark level of the ${}^4I_{13/2}$ state, and g_i is the degeneracy of the *i*th Stark level. When the number of the Stark levels is $m+1$, we have $\sum_{i=0}^m g_i = 14$. The emission spectral distribution function with the normalized area is

$$F(T, \lambda) = A_0 \left[f_0(\lambda) + \sum_{i=1}^m \frac{\gamma_i g_i}{\gamma_0 g_0} e^{-\Delta E_i/kT} f_i(\lambda) \right], \quad (3)$$

with

$$A_0 = \frac{\gamma_0 g_0}{\sum_{i=0}^m \gamma_i g_i e^{-\Delta E_i/kT}}.$$

From Eq. (3), we have

$$\sum_{i=1}^m \frac{\gamma_i g_i e^{-\Delta E_i/kT} f_i(\lambda)}{\gamma_0 g_0} = \frac{F(T, \lambda) - A_0 f_0(\lambda)}{A_0}. \quad (4)$$

The left side of Eq. (4) expresses the spectral components of the emission from the upper Stark levels in the ${}^4I_{13/2}$ state, corresponding to bands *a'* and *b'*, as shown in Fig. 1, the intensity and bandwidth of which have an important effect on the bandwidth of the whole 1.5 μm emission spectra. Before investigating the temperature characteristics of these upper-level emissions, the $f_0(\lambda)$ and A_0 value must be determined first according to the right side of Eq. (4). $f_0(\lambda)$ represents the emission spectra of the transition from the lowest level of the ${}^4I_{13/2}$ state to the ${}^4I_{15/2}$ state. Therefore, the measured emission spectra $F(11 \text{ K}, \lambda)$ at 11 K is reasonably considered as $f_0(\lambda)$ because almost all the populations are populated in the lowest Stark level of the ${}^4I_{13/2}$ state at the low temperature of 11 K. From Eq. (3), A_0 is the composition of $f_0(\lambda)$ in $F(T, \lambda)$, decreasing with the increase of temperature. In Fig. 1, band *b* locates at around 1600 nm far to bands *a'* and *b'*. The overlap of bands *a'* and *b'* with band *b* around the peak position of band *b* ($\lambda_b = 1600 \text{ nm}$) is very small. Thus,

$$f_0(\lambda_b) \approx \sum_{i=1}^m \frac{\gamma_i g_i}{\gamma_0 g_0} e^{-E_i/kT} f_i(\lambda_b)$$

in Eq. (3). The spectral intensity at λ_b [$F(T, \lambda_b)$] is nearly equal to $A_0 f_0(\lambda_b)$. The value of A_0 at a temperature is the proportion of the spectral intensity of band *b* at this temperature to that at the low temperature of 11 K. The values of A_0 at different temperatures are listed in Table I. By using the right side of Eq. (4), the spectral components of the emission from upper Stark levels of the ${}^4I_{13/2}$ state are extracted from the spectra shown in Fig. 1 and plotted in Fig. 2. The spectra exhibit two emission bands *a'* and *b'*. With the increase of temperature, the intensity of bands *a'* and *b'* increase while band *a'* shifts towards the higher energy side of the spectra and band *b'* does not shift. These results indicate that band *a'* is the overlap of the emissions from all upper Stark levels and band *b'* is the emission from a single upper Stark level of the ${}^4I_{13/2}$ state.

Figure 3 shows the temperature dependence of the integrated intensity for spectral bands *a'* and *b'*. After fitting the experimental data by the $\sim e^{-\Delta E/kT}$ term as a thermal activation process, the obtained values of ΔE for bands *a'* and

TABLE I. Values of A_0 at different temperatures.

Temperature (K)	11	40	70	100	150	200	250	300
A_0	1	0.9921	0.9461	0.8562	0.7571	0.6983	0.6933	0.6813

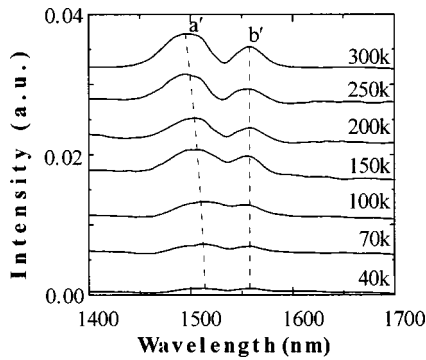


FIG. 2. Emission spectra of the higher levels in the ${}^4I_{13/2}$ state at different temperatures.

b' are 83 and 70 cm^{-1} , respectively. The values show that the effective heights of the upper Stark levels responsible for bands a' and b' are not much different.

In Fig. 1, we see the spectral bandwidth increases with the increase of the composition of the components from the upper Stark levels of the ${}^4I_{13/2}$ state. The dependence of the FWHM on $1-A_0$ is shown in Fig. 4, where $1-A_0$ is considered to be the composition of the components from the upper Stark levels of the ${}^4I_{13/2}$ state because A_0 is defined as the composition of the components from the lowest Stark levels of the ${}^4I_{13/2}$ state. We observe from Fig. 4 that the FWHM increases rapidly as $1-A_0$ is more than 0.3 . If temperature and the extent of Stark splittings remain unchanged, the effective way to obtain a larger value of $1-A_0$ is to increase the spontaneous emission rates of the upper Stark levels of the ${}^4I_{13/2}$ state as described by Eq. (3). Thus, it is concluded that to search for a host with higher spontaneous emission probability of the upper Stark levels of the ${}^4I_{13/2}$ state is very important to broadening of the $1.5\text{ }\mu\text{m}$ emission band.

B. Equivalent model of the four-level system

In Fig. 1, we also note that the energy separation between bands a' and b' is approximately the same as that between bands a and b . Bands $a(a')$ and $b(b')$ exhibit that the ${}^4I_{15/2}$ state may be treated as a two-Stark-level system. Bands $a(b)$ and $a'(b')$ exhibit that the ${}^4I_{13/2}$ state may be also treated as a two-Stark-level system. Then, there is an

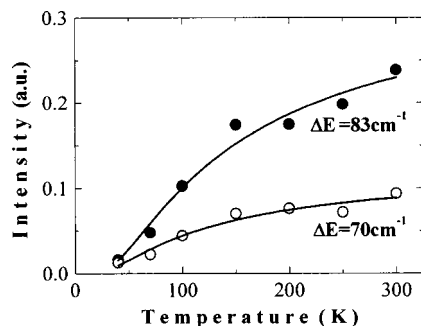


FIG. 3. Temperature dependence of integrated intensity for spectral band a' (●) and b' (○). Experimental data points are fitted by using $\sim e^{-\Delta E/kT}$ as a thermal activation process. The obtained ΔE values for bands a' and b' are 83 and 70 cm^{-1} , respectively.

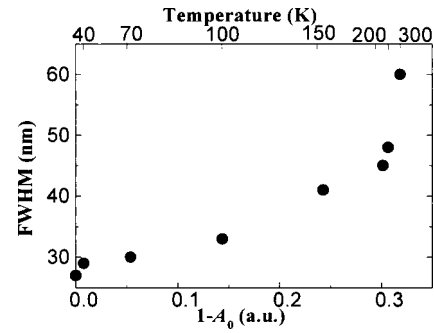


FIG. 4. Dependence of FWHM on the composition ($1-A_0$) of the spectral components from the upper Stark levels of the ${}^4I_{13/2}$ state.

equivalent model of the four-level system for describing the $1.5\text{ }\mu\text{m}$ emission of Er^{3+} ions, as shown in Fig. 5, where all upper Stark levels are treated as one equivalent level except for the lowest level. In Fig. 5, the ${}^4I_{13/2}$ states are composed of the lowest Stark level, labeled by 0 and a set of upper levels, labeled by 1 , and the ${}^4I_{15/2}$ states are composed of a level $0'$ and a set of upper levels $1'$. Bands a and b correspond to the $0-0'$ and $0-1'$ transitions, respectively. Bands a' and b' correspond to the $1-0'$ and $1-1'$ transitions, respectively.

C. Absorption and stimulated-emission cross sections

The absorption cross section is obtained by using absorption spectra of the sample. According to the theory of McCumber,¹⁰ the stimulated-emission cross sections are calculated by using expression (5):

$$\sigma_e(\lambda) = \sigma_a(\lambda) \exp\left[\left(E - \frac{hc}{\lambda}\right)/kT\right], \quad (5)$$

where $\sigma_a(\lambda)$ is the absorption cross section of the transition from the ${}^4I_{15/2}$ state to the ${}^4I_{13/2}$ state, E is the temperature-dependent excitation energy, k is the Boltzman constant, and T is the temperature of the sample.

The shape of the stimulated-emission cross-section spectrum can be also obtained using the measured emission spectrum modified by

$$\sigma_e = \frac{1}{8\pi n^2 c} A \lambda^4 g(\lambda), \quad (6)$$

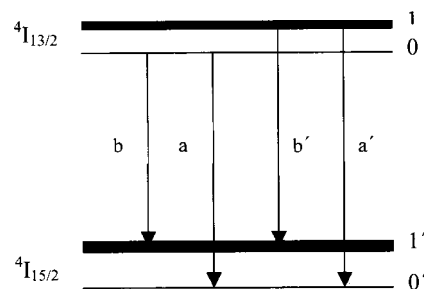


FIG. 5. Equivalent model of the four-level system for describing the $1.5\text{ }\mu\text{m}$ emission of Er^{3+} ions.

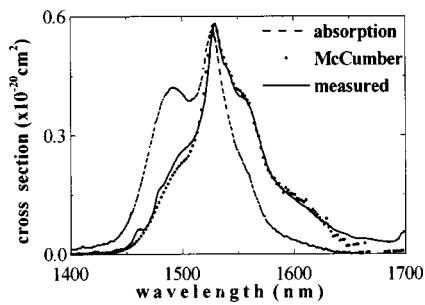


FIG. 6. Absorption and stimulated emission cross-section spectra of the sample.

where n is the refractive index, A is the spontaneous emission probability, and $g(\lambda)$ is the distributing function of the emission spectra. Figure 6 shows the absorption and stimulated emission cross-section spectra. The shape of the emission cross-section spectrum calculated by using the theory of McCumber fits well to that experimentally measured. The absorption and stimulated-emission cross sections are 0.56×10^{-20} and $0.57 \times 10^{-20} \text{ cm}^2$ at a peak of $\lambda_0 = 1526.8 \text{ nm}$, respectively.

IV. CONCLUSIONS

The $1.5 \mu\text{m}$ emission spectra in the Er^{3+} -doped oxide glass are composed of four emission bands, which may be described by an equivalent model of a four-level system. Both the $^4I_{15/2}$ and $^4I_{13/2}$ state multiplets can be considered as a two-level system. Bands a and b are the transition from the

lowest Stark level of the $^4I_{13/2}$ state to the lowest and upper Stark levels of the ground state, respectively. Bands a' and b' are the transition from the upper Stark levels of the $^4I_{13/2}$ state to the lowest and upper Stark levels of the ground state, respectively. To search for a host with higher spontaneous emission probability of the upper Stark levels of the $^4I_{13/2}$ state for Er^{3+} ions is very important to broadening of the $1.5 \mu\text{m}$ emission band of Er^{3+} .

ACKNOWLEDGMENTS

The authors acknowledge support by the National Natural Science Foundation of China under Grant No. 90201010 and the Natural Science Foundation of Jilin Province, China, under Grant No. 20010581.

- ¹S. Tanabe, T. Ohyagi, N. Soga, and T. Hanada, *Phys. Rev. B* **46**, 3305 (1992).
- ²C. D. Ronarch, D. Bayart, Y. Sorel, L. Hamon, M. Guibert, J. L. Beylat, J. F. Kerdiles, and M. Semenkoff, *IEEE Photonics Technol. Lett.* **2**, 509 (1994).
- ³A. Mori, Y. Ohishi, and S. Sudo, *Electron. Lett.* **33**, 863 (1997).
- ⁴A. Jha, S. Shen, and M. Naftaly, *Phys. Rev. B* **62**, 6215 (2000).
- ⁵S. Tanabe, N. Sugimoto, S. Ito, and T. Hanada, *J. Lumin.* **87-89**, 670 (2000).
- ⁶Y. D. Huang, M. Motier, and F. Auzel, *Opt. Mater. (Amsterdam, Neth.)* **15**, 243 (2001).
- ⁷X. Feng, S. Tanabe, and T. Hanada, *J. Appl. Phys.* **89**, 3560 (2001).
- ⁸A. Mori, T. Sakamoto, K. Kodayashi, K. Shikano, and K. Oikawa, *J. Lightwave Technol.* **20**, 822 (2002).
- ⁹V. K. Tikhomirov, D. Furniss, A. B. Seddon, I. M. Reaney, M. Beggiora, M. Ferrari, M. Montagna, and R. Rolli, *Appl. Phys. Lett.* **81**, 1937 (2002).
- ¹⁰W. J. Minsicalco and R. S. Quimby, *Opt. Lett.* **16**, 258 (1991).